Title

Spinal Cord Perfusion MR Imaging Implicates Both Ischemia and Hypoxia in the Pathogenesis of Cervical Spondylosis

Authors

Ellingson, Benjamin M
Woodworth, Davis C
Leu, Kevin
et al.

Publication Date

2019-08-01

DOI

10.1016/j.wneu.2019.04.253

Peer reviewed

HHS Public Access

Author manuscript

World Neurosurg. Author manuscript; available in PMC 2022 February 01.

Published in final edited form as:

World Neurosurg. 2019 August ; 128: e773–e781. doi:10.1016/j.wneu.2019.04.253.

Spinal cord perfusion MR imaging implicates both ischemia and hypoxia in the pathogenesis of cervical spondylosis

Benjamin M. Ellingson, Ph.D.[1,2,4], **Davis C. Woodworth, Ph.D.**[1,2], **Kevin Leu, Ph.D.**[1], **Noriko Salamon, M.D., Ph.D.**[1], **Langston T. Holly, M.D.**[3]

[1]Dept. of Radiological Sciences, David Geffen School of Medicine, University of California Los Angeles, Los Angeles, CA

[2]Dept. of Physics and Biology in Medicine, David Geffen School of Medicine, University of California Los Angeles, Los Angeles, CA

[3]Dept. of Neurosurgery, David Geffen School of Medicine, University of California Los Angeles, Los Angeles, CA

[4]Dept. of Psychiatry and Biobehavioral Sciences, David Geffen School of Medicine, University of California Los Angeles, Los Angeles, CA

Abstract

Objectives: Although a number of studies have implicated ischemia and hypoxia in the pathogenesis of cervical spondylosis (CS), quantification remains difficult and the role of ischemia and hypoxia on disease progression and disease severity in human CS remains largely unknown.

Therefore, the objective of this study was to assess spinal cord perfusion and oxygenation in human CS and examine the relationship between perfusion, degree of spinal cord compression, and neurological status.

Methods: Twenty-two patients with cervical spondylosis with or without myelopathy received a dynamic susceptibility contrast (DSC) perfusion MRI exam consisting of a novel spin-and-gradient echo echoplanar (SAGE-EPI) acquisition before, during, and following gadolinium-based contrast injection. Estimation of relative spinal cord blood volume (rSCBV), the reversible relaxation rate (R_2'), and relative oxygen extraction fraction (rOEF=R_2'/rSCBV) was performed at the site of compression and compared with anterior-posterior spinal cord diameter and mJOA, a measure of neurological impairment.

Results: rSCBV was linearly correlated with both anterior-posterior cord diameter (R^2*=0.4667, P=0.0005*) and mJOA (R^2*=0.2274, P=0.0248*). R_2' was linearly correlated with mJOA (R^2*=0.3998, P=0.0016*) but not cord diameter (R^2*=0.055; P=0.2950*). Also, rOEF was correlated with both cord diameter (R^2*= 0.3440, P=0.0041*) and mJOA (R^2*=0.4699, P=0.0004*).

Address Correspondence To: Benjamin M. Ellingson, Ph.D., Associate Professor of Radiology, Biomedical Physics, Bioengineering, and Psychiatry, Departments of Radiological Sciences and Psychiatry, David Geffen School of Medicine, University of California – Los Angeles, 924 Westwood Blvd, Suite 615, Los Angeles, CA 90024.

Conflicts of Interest: None

Conclusions: Results support the hypothesis that spinal cord compression results in ischemia and hypoxia, and the degree of ischemia and hypoxia is proportional to the degree of neurological impairment.

INTRODUCTION

Cervical spondylosis (CS) is a potentially devastating neurological condition, and the most common cause of spinal cord impairment in older patients. [1–3] Although it is well established that CS is caused by both primary mechanical and secondary biological injury[5,6], some critical questions remain regarding the specific cellular changes that occur during disease pathogenesis. Most notably, despite being hypothesized as a critical pathophysiological mechanism in CS [4], spinal cord ischemia has not been directly observed or quantified *in vivo* in CS patients. A number of studies have documented histological changes [4–7] and angiography data [8,9] in CS consistent with ischemia, and experimental work using animal or preclinical models has demonstrated indirect evidence of ischemia [10,11]. However, quantification of ischemia and hypoxia in CS remains elusive, and the potential role of spinal cord ischemia and hypoxia on disease progression and severity is prime for investigation.

In the current study, we use a novel approach to simultaneously estimate relative spinal cord blood volume (rSCBV) in CS at the site of compression, then measure hypoxia through relative oxygen extraction fraction (rOEF) by quantifying the MR "reversible transverse relaxation rate" (R_2'), which is the basis for blood oxygen level dependent (BOLD) functional imaging [12], has been shown to be proportional to oxygen extraction [13–15], and has been used to characterize hypoxia in both human brain tumors [16,17]and stroke [18,19]. The goal of this investigation was to assess spinal cord perfusion in CS patients and examine the relationship between perfusion, degree of spinal cord compression, and neurological status.

METHODS

Patient Population

A total of 22 patients with cervical spondylosis with or without myelopathy were prospectively enrolled in a cross-sectional study involving advanced MRI and evaluation of neurological function. Patients were recruited from an outpatient neurosurgery clinic, and each had at least moderate cervical stenosis on standard cervical MRI, defined as no visible cerebrospinal fluid signal around the spinal cord at the site of maximal compression. All patients signed Institutional Review Board (IRB) approved consent forms, and all analyses were done in compliance with the Health Insurance Portability and Accountability Act (HIPAA). The cohort included 19 males and 3 females, with a mean age of 56 years old (range = 40–73 years old). The modified Japanese Orthopedic Association (mJOA) score was used as a measure of neurological function[20]. The mean mJOA score for the patient cohort was 15.4 (range= 10 to 18). Additionally, anterior-posterior cord diameter was measured on anatomic images to quantify the degree of cord compression. Mean diameter was approximately 5.1mm and the range was between 3.3mm and 7.8mm. Supplementary patient information is summarized in Table 1.

Conventional Magnetic Resonance Imaging

MRI was obtained on a 3T MR scanner (3T Prisma; Siemens Healthcare, Erlangen, Germany) using a standard spine coil array for radiofrequency reception. Routine clinical MRI scans consisted of T1-weighted and T2-weighted sequences in the sagittal plane and T2-weighted images in the axial orientation. All patients had radiographic evidence of stenosis, including spinal canal narrowing related to advanced cervical spondylosis manifested by a combination of facet arthropathy, ligamentum flavum hypertrophy, and varying degrees of ventral disc-osteophyte compression.

Dynamic Susceptibility Contrast (DSC) Perfusion Imaging Using Multi-Echo Spin-and-Gradient Echo Echoplanar Imaging (SAGE-EPI)

Dynamic susceptibility contrast (DSC) perfusion imaging was collected using a custom SAGE-EPI MRI sequence before, during, and after contrast injection (Fig. 1A). To accomplish this, SAGE-EPI was initiated 15 seconds (10 time points) prior to an injected bolus dose of 0.1 mmol/kg of Gd-DTPA infused at a rate of 3–5 mL/sec and up to 2 minutes following injection and saline flush. The SAGE-EPI readout consisted of two gradient echoes (TE_1=14.0ms; TE_2=34.1ms), an asymmetric spin echo (TE_3= 58.0ms) and a spin echo (TE_4=92.4ms) EPI train in order to acquire quantitative estimates of transverse MR relaxation rates. The repetition time was 1500ms with a slice thickness of $5 mm$ and no additional spacing between slices. The resolution was set to $1.875 \times 1.875 mm$ (in-plane) with a total matrix size of $240 \times 240 mm$. The total number of repetitions (temporal time points) was 120 and were isolated to 23 axial slices through the site of compression.

Perfusion Post-Processing

Dynamic perfusion data were first motion corrected using FSL (FMRIB; https://fsl.fmrib.ox.ac.uk/fsl/; *"mcflirt"*). Then, regions of interest were drawn around the spinal cord at the sites of maximum compression (Fig. 1B). All voxels with temporal signal-to-noise ratio (TSNR) greater than 10 were included to isolate the spinal cord on the motion-corrected T2-weighted echo (TE_2=34.1ms) and averaged together (Fig. 1C-D). Next, $\Delta R_2^*(t)$, the dynamic change in transverse relaxation rate, was calculated as: $\Delta R_2^*(t) = -(TE_2)^{-1} ln(S(t)/S(0))$ using the average temporal dataset from the 2nd echo from the dynamic SAGE-EPI time series data within the area of compression, where TE_2 is the echo time from the 2nd echo, $S(t)$ is MR signal intensity over time, and $S(0)$ is the baseline MR signal intensity prior to contrast administration (Fig. 1E). Lastly, a gamma-variate function was fit to the resulting DSC perfusion time-series data in the form[21,22]:

$$\Delta \widetilde{R}_2^*(t) = A \cdot (t - t_0)^{\alpha} \cdot e^{-\frac{(t - t_0)}{\beta}}; t > t_0 \quad \text{(Eq. 1)}$$

Where A is a scaling factor, a and b determine the bolus shape, and t_0 is the bolus arrival time. Lastly, relative spinal cord blood volume (rSCBV) was estimated by integrating the resulting gamma-variate model fit to $\Delta R_2^*(t)$ time series (Fig. 1E).

$$rSCBV = \int \Delta \widetilde{R}_2^*(t)dt \quad \text{(Eq. 2)}$$

Estimation of Hypoxia and Oxygen Extraction Using R_2' from SAGE-EPI Baseline and rSCBV

Within the same ROI (Fig. 1B), measurements of R_2* and R_2 were performed by averaging the SAGE-EPI data acquired prior to and following bolus injection of gadolinium (Fig. 1D). Data from all four echoes (Fig. 2) were used to estimate R_2* and R_2, which represent the change in the transverse relaxation rates, by solving the following linear equation[27]:

$$\mathbf{A} = \mathbf{Y}^{-1}\mathbf{S} \quad \text{(Eq. 3)}$$

where

$$S = \begin{pmatrix} \ln(S_1) \\ \ln(S_2) \\ \ln(S_3) \\ \ln(S_4) \end{pmatrix}, \mathbf{Y} = \begin{pmatrix} 1 & 0 & -TE_1 & 0 \\ 1 & 0 & -TE_2 & 0 \\ 1 & -1 & -TE_4 + TE_3 & TE_4 - 2 \cdot TE_3 \\ 1 & -1 & 0 & -TE_4 \end{pmatrix}, \mathbf{A} = \begin{pmatrix} \ln(S_0) \\ \ln(\delta) \\ R_2^* \\ R_2 \end{pmatrix} \quad \text{(Eq. 4)}$$

where S_n is signal magnitude for the n^{th} echo and δ is the differences in residual signal differences introduced from imperfectly matched slice profiles. Average R_2' was then estimated using $R_{2'} = R_2* - R_2$. Lastly, the relative oxygen extraction fraction (rOEF) was estimated as:

$$rOEF \propto \frac{R_2'}{rSCBV} \quad \text{(Eq. 5)}$$

as *rOEF* has been shown to be proportional the ratio of R_2' to *rSCBV*[14,15,23].

Statistical Analysis

As described above, the average *rSCBV*, R_2' and *rOEF* extracted from ROIs drawn around the spinal cord at the sites of maximum compression for each patient were measured. A student's t-test was used to test whether *rSCBV*, R_2' and *rOEF* were significantly different in patinets with T2 hyperintensity within the cord at the site of compression. Pearson's correlation coefficient was used to test the hypothesis that *rSCBV*, R_2' and *rOEF* were linearly correlated with the degree of compression estimated from measures of anterior-posterior spinal cord diameter and measures of mJOA. An *F*-test was used to determine whether the slope of the line represented by this correlation was significantly different from zero. *P*-values less than 0.05 were considered statistically significant. GraphPad Prism 7.0d was used for statistical comparisons (GraphPad Software, La Jolla, CA).

RESULTS

The observational data suggested patients with a lesser degree of compression and better neurological function tended to have higher estimates of rSCBV (Fig. 3A-B) and lower estimates of R_2', suggesting patients with significant compression and functional deficits may have more ischemia (lower rSCBV) and hypoxia (higher R_2'), respectively. Fig. 3A-C illustrates sagittal T2-weighted images, axial T2-weighted images at the site of compression, and average DSC perfusion time series in a neurologically intact 52-year-old female CS patient with no functional deficits. In contrast, Fig. 3D-F illustrates similar images and average DSC perfusion time series in a 67-year-old female CS patient with neurological deficits, a high degree of cord compression, and an mJOA score of 10. The area under the DSC perfusion time curve, or rSCBV, is smaller in the patient with high cord compression.

Quantitative measurements of individual patients suggested patients with lower spinal cord volume (rSCBV) had higher degrees of compression (Fig. 4A; $R^2=0.4667$, $P=0.0005$), as measured by anterior-posterior cord diameter, and lower mJOA scores (Fig. 4B; $R^2=0.2274$, $P=0.0248$). No significant association was observed between R_2' and degree of spinal cord compression as estimated by anterior-posterior cord diameter (Fig. 4C; $R^2=0.055$; $P=0.2950$); however, patients with higher measurements of R_2', suggesting more hypoxia, appeared to have lower mJOA (Fig. 4D; $R^2=0.3998$, $P=0.0016$).

Oxygen extraction (*rOEF)* was estimated using both R_2' and *rSCBV* and correlated with cord compression, and mJOA score. A statistically significant correlation was observed between *rOEF* and anterior-posterior cord diameter (Fig. 4E; $R^2= 0.3440$, $P=0.0041$). Additionally, a strong significant correlation was observed between *rOEF* and mJOA (Fig. 4F; $R^2=0.4699$, $P=0.0004$), implying patients with higher oxygen extraction at the site of compression may suffer from worse neurological function.

A total of 17 of the 22 patients (77%) exhibited some degree of T2 hyperintensity within the spinal cord at the site of compression. No significant difference in rSCBV was observed in patients with T2 hyperintensity ($P=0.5756$), although patients with T2 signal change tended to have slightly (~8%) lower relative blood volume. Virtually no difference in R_2' was observed between patients with T2 signal change within the cord and those with normal signal intensity ($P=0.9651$). Similarly, measures of rOEF were not significantly different between patients with and without T2 signal change ($P=0.6034$), but patients with signal change tended to have slightly higher (~10%) relative oxygen extraction fraction.

DISCUSSION

There is mounting evidence from both post mortem human and animal model investigations that ischemia plays a significant role in CS pathogenesis, yet direct demonstration of this mechanism in vivo has been elusive to date. Human histopathological autopsy studies have demonstrated a consistent pattern of deleterious changes including cystic cavitation and focal necrosis in the central gray and white matter that progresses to lacunae, gliosis, and anterior horn dropout[24]. These findings are consistent with animal studies that have demonstrated that anterior-posterior spinal cord compression results in

decreased blood flow to the compressed spinal segment [25]. The decrease in microcirculation blood flow is postulated to be caused by obstruction of the anterior sulcal arteries and transversely coursing arteries in the central gray matter [9,26]. Additional sources of ischemia include impairment of the radiculomedullary arterial diameter by a sufficiently narrowed intervertebral foramen[5] and vessel wall thickening and hyalinization in the anterior spinal artery and parenchymal arterioles [4,6]. These findings have been supported by MR spectroscopic imaging studies showing lactate peaks in the spinal cord spectra of CS patients[27], a sign of anaerobic metabolism providing cellular biochemical evidence of spinal cord ischemia.

In contrast to the spinal cord, both blood flow and tissue oxygen demand have been well studied elsewhere in the CNS. Cerebral autoregulation is modulated by many factors, with the ultimate goal of maintaining cerebral perfusion and preservation of tissue oxygenation. Cerebral blood flow measurements play a vital role in the treatment of a variety of neurological disorders that affect the brain including stroke[21,22], subarachnoid hemorrhage [28], and traumatic brain injury[29]. The ability to successfully and reliably measure cerebral blood flow has revolutionized the manner in which these conditions are treated and greatly improved outcomes.

The present study has elucidated a number of novel findings in the assessment of CS patients. We found a strong correlation between decreased anterior-posterior diameter of the spinal cord and decreased spinal cord blood volume. This is consistent with animal studies that demonstrated that spinal cord compression is associated with decreased spinal cord blood flow. The exact source of compromised flow in the human spinal cord microcirculation is beyond the scope of our study, yet based on animal studies it is most likely due to compression of the anterior sulcal and grey matter arteries. Another previously undescribed finding is the statistically significant relationship between spinal cord blood flow and neurological status, as measured by the mJOA score. This result further highlights the role of ischemia in CS pathogenesis.

Consistent with the aforementioned relationship between spinal cord ischemia and neurological function, a higher degree of hypoxia as measured by R_2' was similarly associated with a poorer neurological function. However, in contrast to spinal cord ischemia, spinal cord hypoxia was not statistically correlated with the degree of spinal cord compression. On first glance this finding may appear to be inconsistent with the premise that compromised blood flow is a major component of CS pathogenesis. However, this difference in the relationship between ischemia/hypoxia and spinal cord diameter can be explained by the spinal cord oxygen extraction measurements *(rOEF*). The degree of spinal cord oxygen extraction was significantly correlated with anterior-posterior spinal cord diameter. Of all the measurements performed in this study, the strongest correlation was between oxygen extraction and mJOA score, indicating that patients with a higher oxygen extraction have worse neurological function. Thus, although a decreased spinal cord diameter was associated with decreased blood flow, the determination of spinal cord hypoxia is in part dependent on the ability of the tissue to extract oxygen. As the spinal cord becomes more compressed and blood flow decreases, there is an apparent stimulus to extract more oxygen from the compromised vasculature, likely as a method to prevent hypoxia in the face of ischemia.

These alterations in spinal cord oxygen extraction, along with autoregulation, can be considered a compensatory mechanism designed to maintain tissue perfusion, and equivalent mechanisms have been extensively studied in the brain. It is believed autoregulation, which causes an increase in cerebral blood flow via vasodilation of resistance arterioles, is the initial compensatory mechanism employed during a significant decrease of cerebral perfusion pressure[30]. Once autoregulation is exhausted due to a critical reduction of cerebral perfusion pressure, and cerebral blood flow further falls, increases in cerebral oxygen extraction are utilized to maintain cerebral oxygen metabolism. An argument can be made that a reduction of spinal cord blood flow by direct compression and chronic vessel wall injury can similarly lead to compensatory increases in spinal cord oxygen extraction. It is very likely that ischemia and spinal cord compression work synergistically in the pathogenesis of CS and should not be evaluated in isolation. In an experimental model of compression myelopathy using dogs, Gooding *et al.*[11] demonstrated that the neurological sequelae of spinal cord ischemia appear additive to that of compression, such that ischemia and compression cause a greater degree of impairment than either mechanism alone.

In addition to CS, there are other potential applications for spinal cord perfusion imaging. There has been increasing interest in the assessment, and potential treatment of increased intraspinal pressure following acute traumatic spine injury, with the ultimate goal of preventing spinal cord ischemia and further injury, akin to that following traumatic brain injury. Several different methodologies have been advocated to measure and treat increased intrapsinal pressure including subdural probes [31–33]and lumbar drainage [34,35]. Although these specific techniques have not been universally adopted, the concept of preventing or minimizing spinal cord ischemia following traumatic SCI with techniques such as hypertensive therapy [36] are widely accepted, and the ability to measure spinal cord perfusion parameters such as blood flow and oxygen extraction could be a helpful addition to our diagnostic and therapeutic armamentarium. Similar benefits could be actualized in the management of other etiologies of spinal cord ischemia such as those with presumed vascular insufficiency following abdominal aortic repair [37,38], that may undergo prophylactic or postoperative lumbar drain placement to diminish intraspinal pressure.

While dynamic contrast enhanced (DCE) perfusion MRI has been performed to evaluate blood spinal cord barrier integrity[39,40], to our best knowledge, the present study is the first to successfully estimate relative spinal cord blood volume and oxygen extraction in human patients with CS using dynamic susceptibility contrast (DSC) perfusion MRI. DSC-MRI relies on fast imaging techniques to image the first past of MR contrast as it travels through the vasculature to estimate blood volume and flow. Because of the significant magnetic susceptibility gradients present around the spinal cord due to the nearby presence of bone and CSF, combined with the relatively small size and potential motion of the cord, common techniques for brain perfusion imaging (e.g. echoplanar imaging) are challenging. Due to the difficulties with image artifacts, we chose to pool voxel data with high signal-to-noise (SNR) inside the spinal cord throughout the site of compression for each patient, then use these values as an estimate of spinal cord perfusion at the site of injury. Future studies aimed at further improving the SNR and reducing susceptibility-related image distortion will allow for maps of localized changes in blood perfusion in the spinal cord; however, this remains difficult given current technology.

The present study largely serves as an initial proof of concept investigation, and is the first to directly link spinal cord hypoxia and ischemia to degree of impairment in CS patients. Two potential applications of this technology include the use of perfusion imaging to assess disease progression in non-operatively treated patients, as well as the ability of perfusion imaging to predict outcome following surgical decompression. Both of these applications were beyond the scope of this initial investigation but will be assessed in future studies.

CONCLUSIONS

In summary, results from the current study support the hypothesis that spinal cord compression due to CS may result in both cord ischemia and hypoxia, and the degree of ischemia and hypoxia at the site of compression appears proportional to the degree of neurological impairment.

Acknowledgments

Research Support: Funding was received through the following NIH/NINDS grants: no. 2R01NS078494-06 (to LTH, NS, and BME)

REFERENCES

1. Montgomery DM, Brower RS. Cervical spondylotic myelopathy. Clinical syndrome and natural history. Orthop Clin North Am. 1992;23(3):487–493. [PubMed: 1620540]
2. Wilkinson M. The morbid anatomy of cervical spondylosis and myelopathy. Brain. 1960;83:589–617. [PubMed: 13785329]
3. Young WF. Cervical spondylotic myelopathy: a common cause of spinal cord dysfunction in older persons. Am Fam Physician. 2000;62(5):1064–1070, 1073. [PubMed: 10997531]
4. Brain WR, Knight GC, Bull JW. Discussion of rupture of the intervertebral disc in the cervical region. Proc R Soc Med. 1948;41(8):509–516. [PubMed: 18877123]
5. Taylor AR. Mechanism and treatment of spinal-cord disorders associated with cervical spondylosis. Lancet. 1953;1(6763):717–720. [PubMed: 13036140]
6. Mair WG, Druckman R. The pathology of spinal cord lesions and their relation to the clinical features in protrusion of cervical intervertebral discs; a report of four cases. Brain. 1953;76(1):70–91. [PubMed: 13041923]
7. Breig A, Turnbull I, Hassler O. Effects of mechanical stresses on the spinal cord in cervical spondylosis. A study on fresh cadaver material. J Neurosurg. 1966;25(1):45–56. [PubMed: 5947047]
8. Strek P, Reron E, Maga P, Modrzejewski M, Szybist N. A possible correlation between vertebral artery insufficiency and degenerative changes in the cervical spine. Eur Arch Otorhinolaryngol. 1998;255(9):437–440. [PubMed: 9833209]
9. Doppman JL. The mechanism of ischemia in anteroposterior compression of the spinal cord. Invest Radiol. 1975;10(6):543–551. [PubMed: 811584]
10. Gooding MR, Wilson CB, Hoff JT. Experimental cervical myelopathy. Effects of ischemia and compression of the canine cervical spinal cord. J Neurosurg. 1975;43(1):9–17. [PubMed: 1141988]
11. Gooding MR, Wilson CB, Hoff JT. Experimental cervical myelopathy: autoradiographic studies of spinal cord blood flow patterns. Surg Neurol. 1976;5(4):233–239. [PubMed: 1265634]
12. Ogawa S, Lee TM, Kay AR, Tank DW. Brain magnetic resonance imaging with contrast dependent on blood oxygenation. Proc Natl Acad Sci U S A. 1990;87(24):9868–9872. [PubMed: 2124706]
13. An H, Lin W. Quantitative measurements of cerebral blood oxygen saturation using magnetic resonance imaging. J Cereb Blood Flow Metab. 2000;20(8):1225–1236. [PubMed: 10950383]

14. Domsch S, Mie MB, Wenz F, Schad LR. Non-invasive multiparametric qBOLD approach for robust mapping of the oxygen extraction fraction. Z Med Phys. 2014;24(3):231–242. [PubMed: 24743060]
15. He X, Zhu M, Yablonskiy DA. Validation of oxygen extraction fraction measurement by qBOLD technique. Magn Reson Med. 2008;60(4):882–888. [PubMed: 18816808]
16. Harris RJ, Yao J, Chakhoyan A, et al. Simultaneous pH-sensitive and oxygen-sensitive MRI of human gliomas at 3 T using multi-echo amine proton chemical exchange saturation transfer spin-and-gradient echo echo-planar imaging (CEST-SAGE-EPI). Magn Reson Med. 2018.
17. Toth V, Forschler A, Hirsch NM, et al. MR-based hypoxia measures in human glioma. J Neurooncol. 2013;115(2):197–207. [PubMed: 23918147]
18. Geisler BS, Brandhoff F, Fiehler J, et al. Blood-oxygen-level-dependent MRI allows metabolic description of tissue at risk in acute stroke patients. Stroke. 2006;37(7):1778–1784. [PubMed: 16741186]
19. Jensen-Kondering U, Baron JC. Oxygen imaging by MRI: can blood oxygen level-dependent imaging depict the ischemic penumbra? Stroke. 2012;43(8):2264–2269. [PubMed: 22588263]
20. Yonenobu K, Abumi K, Nagata K, Taketomi E, Ueyama K. Interobserver and intraobserver reliability of the japanese orthopaedic association scoring system for evaluation of cervical compression myelopathy. Spine (Phila Pa 1976). 2001;26(17):1890–1894; discussion 1895. [PubMed: 11568701]
21. Davenport R. The derivation of the gamma-variate relationship for tracer dilution curves. J Nucl Med. 1983;24(10):945–948. [PubMed: 6352876]
22. Thompson HK Jr., Starmer CF, Whalen REHD. Indicator Transit Time Considered as a Gamma Variate. Circ Res. 1964;14:502–515. [PubMed: 14169969]
23. Yablonskiy DA, Sukstanskii AL, He X. Blood oxygenation level-dependent (BOLD)-based techniques for the quantification of brain hemodynamic and metabolic properties - theoretical models and experimental approaches. NMR Biomed. 2013;26(8):963–986. [PubMed: 22927123]
24. Henderson FC, Geddes JF, Vaccaro AR, Woodard E, Berry KJ, Benzel EC. Stretch-associated injury in cervical spondylotic myelopathy: new concept and review. Neurosurgery. 2005;56(5):1101–1113; discussion 1101–1113. [PubMed: 15854260]
25. Kurokawa R, Murata H, Ogino M, Ueki K, Kim P. Altered blood flow distribution in the rat spinal cord under chronic compression. Spine (Phila Pa 1976). 2011;36(13):1006–1009. [PubMed: 21192287]
26. Baptiste DC, Fehlings MG. Pathophysiology of cervical myelopathy. Spine J. 2006;6(6 Suppl):190S–197S. [PubMed: 17097538]
27. Holly LT, Freitas B, McArthur DL, Salamon N. Proton magnetic resonance spectroscopy to evaluate spinal cord axonal injury in cervical spondylotic myelopathy. J Neurosurg Spine. 2009;10(3):194–200. [PubMed: 19320577]
28. Grubb RL Jr., Raichle ME, Eichling JO, Gado MH. Effects of subarachnoid hemorrhage on cerebral blood volume, blood flow, and oxygen utilization in humans. J Neurosurg. 1977;46(4):446–453. [PubMed: 845630]
29. Kelly DF, Martin NA, Kordestani R, et al. Cerebral blood flow as a predictor of outcome following traumatic brain injury. J Neurosurg. 1997;86(4):633–641. [PubMed: 9120627]
30. Derdeyn CP, Videen TO, Yundt KD, et al. Variability of cerebral blood volume and oxygen extraction: stages of cerebral haemodynamic impairment revisited. Brain. 2002;125(Pt 3):595–607. [PubMed: 11872616]
31. Phang I, Werndle MC, Saadoun S, et al. Expansion duroplasty improves intraspinal pressure, spinal cord perfusion pressure, and vascular pressure reactivity index in patients with traumatic spinal cord injury: injured spinal cord pressure evaluation study. J Neurotrauma. 2015;32(12):865–874. [PubMed: 25705999]
32. Varsos GV, Werndle MC, Czosnyka ZH, et al. Intraspinal pressure and spinal cord perfusion pressure after spinal cord injury: an observational study. J Neurosurg Spine. 2015;23(6):763–771. [PubMed: 26273764]

33. Werndle MC, Saadoun S, Phang I, et al. Monitoring of spinal cord perfusion pressure in acute spinal cord injury: initial findings of the injured spinal cord pressure evaluation study*. Crit Care Med. 2014;42(3):646–655. [PubMed: 24231762]
34. Squair JW, Belanger LM, Tsang A, et al. Spinal cord perfusion pressure predicts neurologic recovery in acute spinal cord injury. Neurology. 2017;89(16):1660–1667. [PubMed: 28916535]
35. Kwon BK, Curt A, Belanger LM, et al. Intrathecal pressure monitoring and cerebrospinal fluid drainage in acute spinal cord injury: a prospective randomized trial. J Neurosurg Spine. 2009;10(3):181–193. [PubMed: 19320576]
36. Walters BC, Hadley MN, Hurlbert RJ, et al. Guidelines for the management of acute cervical spine and spinal cord injuries: 2013 update. Neurosurgery. 2013;60 Suppl 1:82–91. [PubMed: 23839357]
37. Ackerman LL, Traynelis VC. Treatment of delayed-onset neurological deficit after aortic surgery with lumbar cerebrospinal fluid drainage. Neurosurgery. 2002;51(6):1414–1421; discussion 1421–1412. [PubMed: 12445346]
38. Khan NR, Smalley Z, Nesvick CL, Lee SL, Michael LM, 2nd. The use of lumbar drains in preventing spinal cord injury following thoracoabdominal aortic aneurysm repair: an updated systematic review and meta-analysis. J Neurosurg Spine. 2016;25(3):383–393. [PubMed: 27058497]
39. Bilgen M, Narayana PA. A pharmacokinetic model for quantitative evaluation of spinal cord injury with dynamic contrast-enhanced magnetic resonance imaging. Magn Reson Med. 2001;46:1099–1106. [PubMed: 11746575]
40. Tatar I, Chou PC, Desouki MM, El Sayed H, Bilgen M. Evaluating regional blood spinal cord barrier dysfunction following spinal cord injury using longitudinal dynamic contrast-enhanced MRI. BMC Med Imaging. 2009;9:10. [PubMed: 19519898]

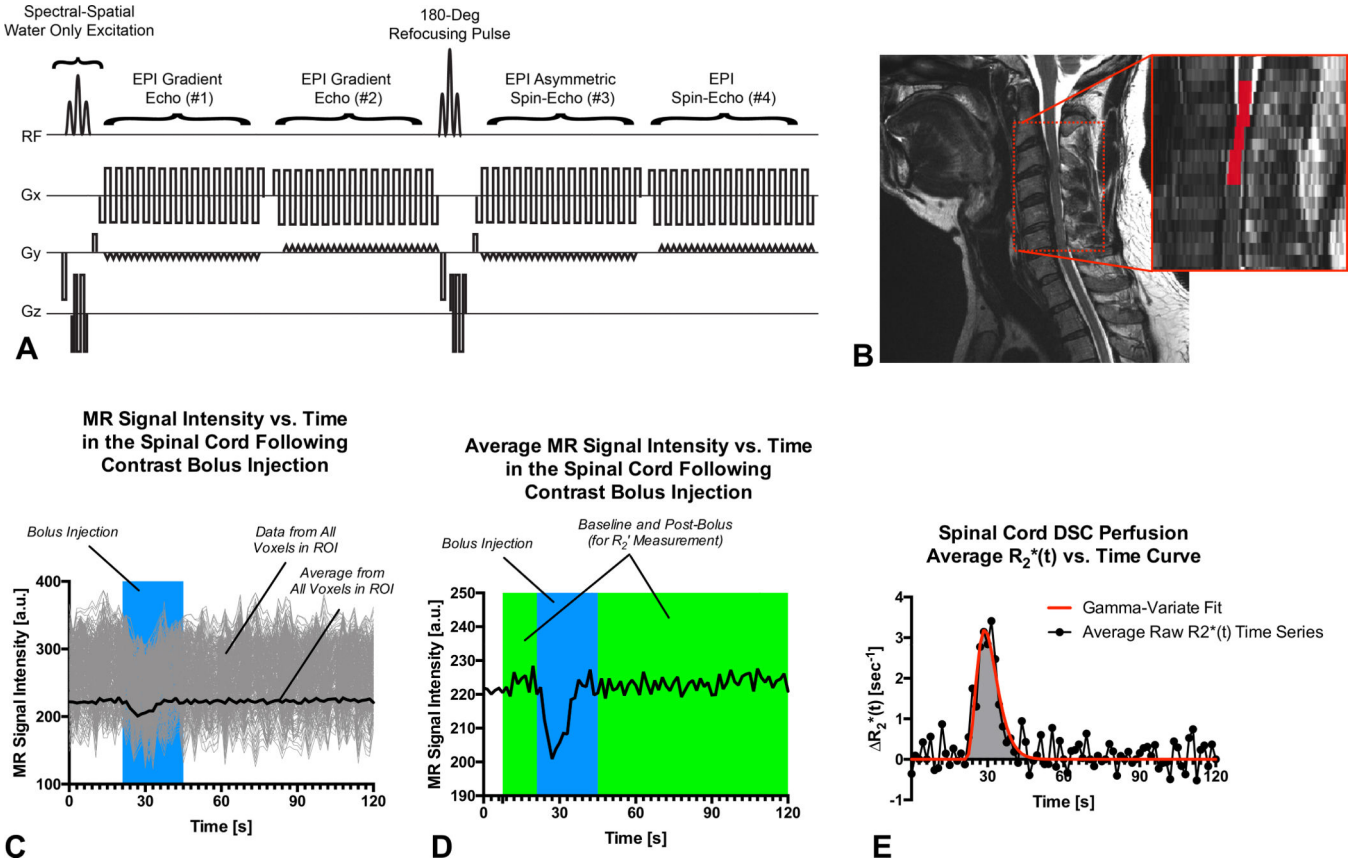

Fig. 1:

A) Spin-and-gradient echo echoplanar imaging (SAGE-EPI) MRI pulse sequence showing acquisition of 4 echoes per repetition time (TR). RF = radiofrequency pulses. Gx, Gy, Gz = gradients applied in the x, y, and z orientation. B) Region of interest (ROI) at the site of compression. C) Diagram depicting MR signal intensity as a function of time for all voxels in the spinal cord at the site of compression following contrast bolus injection (gray lines), window of bolus injection (blue area)), and average MR signal intensity time course (black line). D) Average MR signal intensity versus time (black line) during bolus injection (blue area) along with baseline and post-bolus time periods (green areas) used for R_2' measurement. E) Average transverse relaxation rate as a function of time (R_2*(t)) and gamma-variate fit (red line) used for estimation of relative spinal cord blood volume (rSCBV).

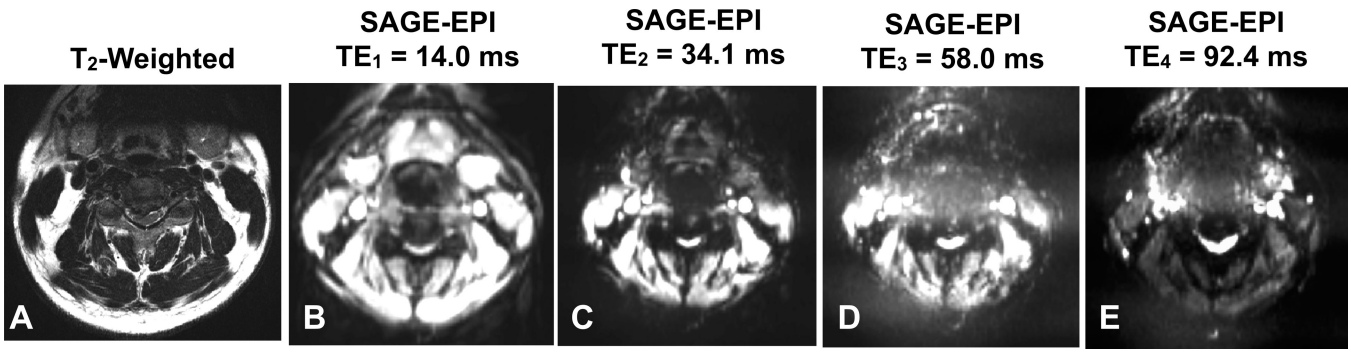

Fig. 2:

A) Axial T2-weighted image and corresponding SAGE-EPI images with B) echo time $(TE)_1$=14.0ms, C) TE_2=34.1ms, D) TE_3=58.0ms, and E) TE_4=92.4ms at the site of compression in a patient with CS.

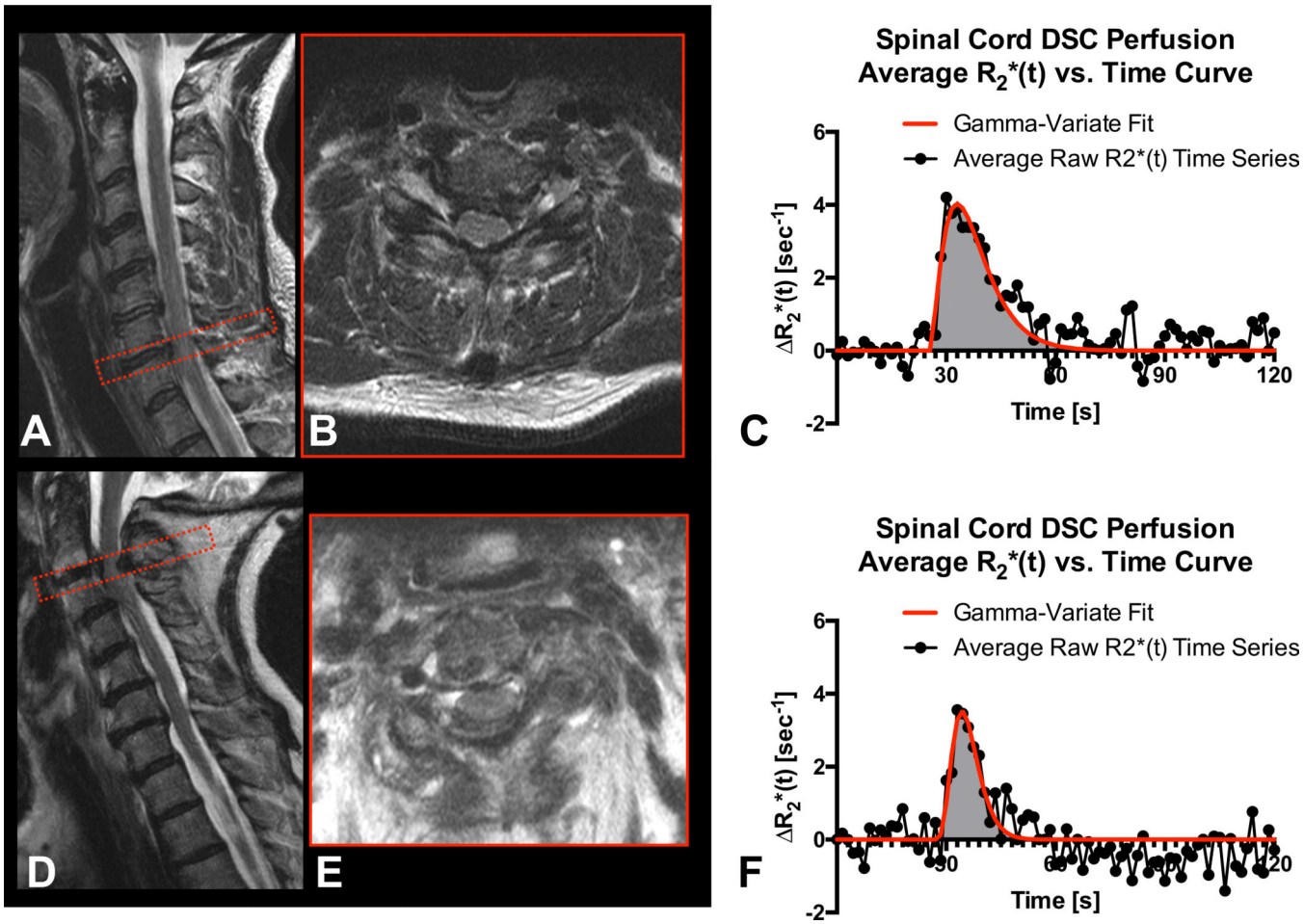

Fig. 3:

A-C) 52-year-old female patient with mJOA=18 and anterior-posterior cord diameter of 5.1*mm*. D-F) 67-year-old female patient with mJOA = 10 and anterior-posterior cord diameter of 4.5*mm*. A,D) A) Sagittal T2-weighted image. B,E) Axial T2-weighted image at the site of compression. C,F) Dynamic transverse relaxation rate ($R_2*(t)$) perfusion time series average raw data (black line) and gamma-variate model fit (red line) during bolus injection.

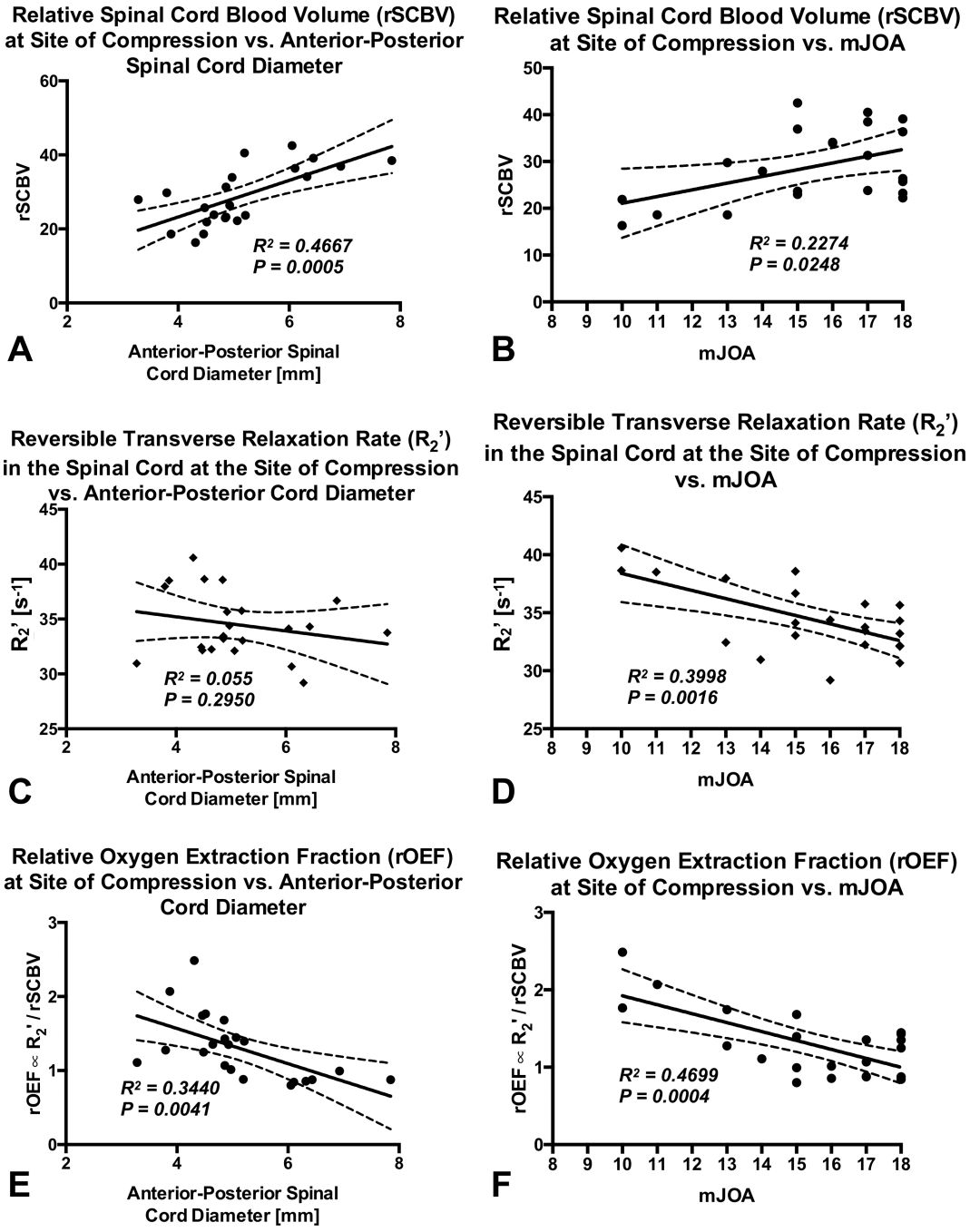

Fig. 4:

Linear correlations between perfusion measures and clinical function at the site of compression: A) relative spinal cord blood volume (rSCBV) and anterior-posterior spinal cord diameter (R^2=0.4667, P=0.0005); B) rSCBV and mJOA (R^2=0.2274, P=0.0248); C) reversible transverse relaxation rate (R_2') and anterior-posterior spinal cord diameter (R^2=0.055, P=0.2950); D) R_2' and mJOA (R^2=0.3998, P=0.0016); E) relative oxygen extraction fraction (*rOEF*) and anterior-posterior cord diameter (R^2=0.3440, P=0.0041); and

F) *rOEF* and mJOA (R^2*=0.4699, P=0.0004*). Solid and dashed lines represent best-fit line and 95% confidence intervals, respectively.

Table 1:

Patient Demographics, Anatomic Imaging, and Perfusion MR Measurements.

Patient Demographics				Anatomic Imaging			Perfusion Quality Control		Perfusion Measurements		
Patient	**Age**	**Sex**	**mJOA**	**SC A-P Diam [mm]**	**L-R Diam [mm]**	**T2 Change**	**AIF Quality**	**rSCBV Quality**	**rSCBV**	**R_2' [s^{-1}]**	**rOEF ~ R_2'/rSCBV**
1	42	M	18	6.1	14.9	Yes	Good	Good	36.37	30.68	0.84
2	61	M	15	5.2	13.1	Yes	Fair	Fair	23.66	33.04	1.40
3	58	F	10	4.3	15.9	Yes	Good	Good	16.33	40.59	2.49
4	59	M	18	4.9	12.3	Yes	Good	Good	26.37	35.66	1.35
5	62	M	15	6.9	14.6	Yes	Fair	Good	36.95	36.68	0.99
6	67	F	10	4.5	11.5	Yes	Good	Good	21.88	38.64	1.77
7	46	M	16	6.3	12.5	Yes	Good	Good	34.12	29.19	0.86
8	65	M	18	6.4	14.5	Yes	Good	Good	39.12	34.31	0.88
9	60	M	17	7.8	14.0	No	Good	Good	38.50	33.76	0.88
10	59	M	17	4.9	12.8	Yes	Good	Fair	31.31	33.43	1.07
11	71	M	18	4.5	15.3	No	Good	Good	25.74	32.16	1.25
12	50	M	16	5.0	13.1	Yes	Good	Good	33.94	34.39	1.01
13	52	F	18	5.1	12.2	Yes	Fair	Fair	22.21	32.12	1.45
14	40	M	15	6.1	16.7	Yes	Good	Good	42.54	34.12	0.80
15	72	M	17	5.2	12.6	No	Good	Good	40.54	35.76	0.88
16	54	M	11	3.9	14.6	Yes	Good	Good	18.60	38.50	2.07
17	55	M	15	4.8	13.4	Yes	Good	Fair	22.96	38.58	1.68
18	46	M	13	4.5	16.0	No	Good	Good	18.61	32.44	1.74
19	50	M	17	4.6	14.0	Yes	Fair	Fair	23.83	32.24	1.35
20	40	M	14	3.3	17.1	Yes	Fair	Fair	27.95	30.96	1.11
21	73	M	13	3.8	13.8	No	Good	Good	29.77	37.98	1.28
22	50	M	18	4.9	19.1	Yes	Fair	Fair	23.24	33.21	1.43

mJOA = modified Japanese Orthopedic Association score. SC = spinal cord. Diam = diameter. AIF = arterial input function. rSCBV = relative spinal cord blood volume. rOEF = relative oxygen extraction fraction. M=male. F=female.4